Shock-Proof Design of Head Disk Assembly Subjected to Impulsive Excitation*

Zhongwei JIANG**, Kazu TAKASHIMA**
and Seiji CHONAN**

This paper reports a study on the transient response of a head disk assembly (HDA) subjected to a half-sine shock pulse in the axial and pitching directions. The solution is obtained using the multi-modal expansion approximation and applying the Galerkin method to the resulting equations. Numerical results are obtained by the Newmark β method for a 3.5″ hard disk-head system. It is found that the relative distance between the head and the disk reduces to the minimum when the input duration τ is about 1.5 times the natural half-period of the fundamental (0, 0) mode. Results obtained also show that the shock-proof head satisfies $(1/2\pi)(k/m)^{1/2}=f_{00}$, where k is the stiffness of the head arm, m the head mass and f_{00} the (0, 0) mode frequency of the rotating disk, and that the head slider should be designed so that the assembled system of the head and the disk has a high air-film stiffness.

Key Words: Vibration of Rotating Body, Transient Response, Natural Frequency, Head Disk Assembly, Half-Sine Shock Pulse, Shock-Proof Design, Galerkin Method, Newmark β Method

1. Introduction

With the development of information-intensive cultures, it has become commonly observed that electronic equipment is subjected to mechanical disturbances. A typical example is a notebook computer which is prone to being knocked, jolted and bumped while being carried. It is therefore of technological importance to investigate the dynamics of such vibration-sensitive systems, to further improve their durability to the dynamic loading.

Limiting the problem to the dynamic response of magnetic disk drives, Ono et al.[1] obtained the deflection of a rotating flexible disk under a stationary concentrated lateral force. Furthermore, Chonan and Jiang[2] and Jiang et al.[3] studied the vibrations of a read/write head floppy disk system subjected to axial and pitching oscillations. Honda et al.[4] calculated the steady-state response of a rotating disk to a concentrated harmonic force. Yano and Kotera[5] investigated the stability of a spinning disk with a stationary spring at the outer periphery. Ono et al.[6], Fukui et al.[7] and Odaka et al.[8] studied the floating clearance between the head slider and the magnetic disk experimentally and theoretically.

Furthermore Chonan et al.[9] studied the shock response of rotating magnetic disks to impulsive loading. It was found that the peak displacement and acceleration that appear on the disk take maxima when the input duration is about 1.5 times the half-period of the fundamental (0, 0) mode of the disk. Furthermore, the shock pulse with a duration 11 ms, which is currently used as a standard input for the shock test of disk drive units, produces only 60 - 70% of the maximum displacement and acceleration that may occur for the rotating disk. In our previous study[9], however, the effect of the floating head was not taken into account in the analysis. In some cases, the head impacts against the disk when the system is excited by an impulsive acceleration, and this damages the data during the process of writing or reading. It is therefore of importance to investigate the dynamics of head-disk systems subjected to impulsive

* Received 19th November, 1993. Japanese original: Trans. Jpn. Soc. Mech. Eng., Vol. 58, No. 556, C (1992), pp. 3681-3688. (Received 27th March, 1992)

** Department of Aeronautics and Space Engineering, Tohoku University, Sendai 980-77, Japan

loading. In this context, the problem discussed in this paper is that of the transient vibrations of the rotating hard disk-floating head system subjected to a half-sine shock pulse in the axial and pitching directions. A solution is obtained by introducing both the Galerkin method in the space domain and the Newmark β method in the time domain.

Nomenclature

a : Outer radius (m)
b : Inner radius (m)
c : Coefficient of viscous damping (s)
D : $Eh^3/12(1-\nu^2)$ Flexural stiffness of disk (N·m)
E : Young's modulus (N/m^2)
G_a, G_p : Acceleration amplitudes in axial and pitching directions (g)
h : Thickness (m)
k : Stiffness of head arm (kg/m)
k_{air} : Stiffness of air film between head and disk (kg/m)
m : Mass of head (kg)
t : Time (s)
u : Displacement of disk in (u, r, η) coordinates (m)
u_H : Displacement of head in (u, r, η) coordinates (m)
$\partial^2 z_{case}/\partial t^2$: External impulsive acceleration to disk case
(u, r, η) : Coordinate frame moving with disk case
ν : Poisson's ratio
ρ : Density (kg/m^3)
σ_r, σ_η : Centrifugal stresses due to the disk rotation (N/m^2)
τ : π/ω Duration of impulsive acceleration (s)
Ω : Revolution speed (rad/s)
ω : Rate of impulsive acceleration (rad/s)

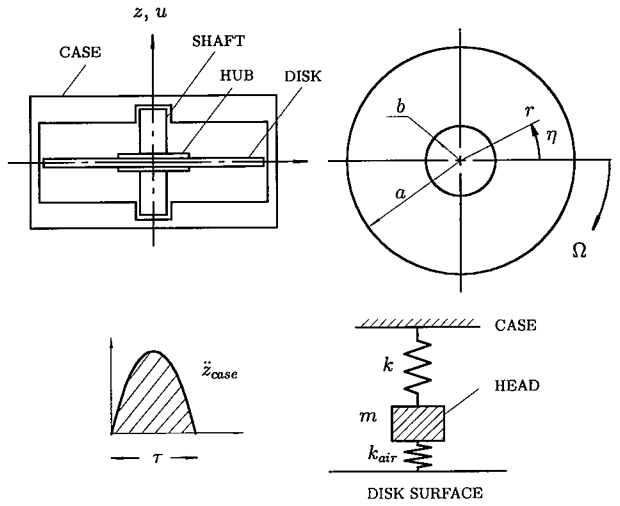

Fig. 1 Geometry of problem and coordinates

2. Formulation of the Problem

Figure 1 shows a hard disk of outer radius a and inner radius b rotating at a constant angular speed Ω in the clockwise direction. The disk unit is excited by an impulsive axial or pitching acceleration $\ddot{z}_{case}$. The R/W head is modelled by a mass-spring system and the air film between the head and the disk is approximated by an elastic foundation of stiffness k_{air}. In the following, one denotes the coordinate frame fixed on the disk case by (u, r, η) and the lateral displacement of the disk in the (u, r, η) frame also by u. In this case, the equation of motion of the disk with respect to the coordinate frame (u, r, η) is

$$D\left[1+c\left(\frac{\partial}{\partial t}-\Omega\frac{\partial}{\partial \eta}\right)\right]\nabla^4 u+\rho h\left(\frac{\partial}{\partial t}-\Omega\frac{\partial}{\partial \eta}\right)^2 u -\frac{h}{r}\frac{\partial}{\partial r}\left(\sigma_r r\frac{\partial u}{\partial \eta}\right)-\frac{h}{r}\frac{\partial}{\partial \eta}\left(\sigma_\eta\frac{\partial u}{r\partial \eta}\right) +k_{air}(u-u_H)\delta(\eta-\eta_0)\frac{\delta(r-\xi)}{r} =-\rho h\frac{\partial^2 z_{case}}{\partial t^2}. \quad (1)$$

The equation of motion of the head is

$$m\frac{\partial^2 u_H}{\partial t^2}+(k+k_{air})u_H-k_{air}u=-m\frac{\partial^2 z_{case}}{\partial t^2}, \quad (2)$$

where $\partial^2 z_{case}/\partial t^2$ is the input acceleration to the disk drive unit. It is assumed that the disk is subjected to a half-sine shock wave pulse in the axial or pitching direction. In this case, the acceleration is written generally in the form

$$\frac{\partial^2 z_{case}}{\partial t^2}=\begin{cases}\left[G_a+G_p\left(\frac{r}{a}\right)\cos\eta\right]\sin\omega t & \text{for } 0\le t\le\tau,\\ 0 & \text{for } \tau<t,\end{cases} \quad (3)$$

where $\tau\ (=\pi/\omega)$ is the duration of the shock pulse and G_a, G_p are the peak accelerations in the axial and pitching directions, respectively.

The solution of Eq.(1) may be written in the form

$$u(r,\eta,t)=\sum_{m=0}^{M}\sum_{n=0}^{N}[C_{mn}(t)\cos(n\eta) +S_{mn}(t)\sin(n\eta)]R_{mn}(r), \quad (4)$$

where $C_{mn}(t)$ and $S_{mn}(t)$ are the time functions determined in the following analysis; m and n are the numbers of nodal circles and diameters on the disk, and M and N the numbers of terms of the series taken into account in the analysis. R_{mn} are space functions satisfying the boundary conditions, which are approximated by the mode functions of a non rotating disk, i.e.,

$$R_{mn}=J_n\left(K_{mn}\frac{r}{a}\right)+F_{mn}Y_n\left(K_{mn}\frac{r}{a}\right)$$

$$+G_{mn}I_n\left(K_{mn}\frac{r}{a}\right)+H_{mn}K_n\left(K_{mn}\frac{r}{a}\right), \tag{5}$$

where J_n and Y_n are Bessel functions and I_n and K_n are modified Bessel functions of order n; F_{mn} through K_{mn} are constants determined from the clamped-free boundary conditions.

Substituting Eq.(4) into Eq.(1), further multiplying the resulting equation by $rR_{ql}(r)\cos(l\eta)\cdot d\eta dr$ and integrating from $r=b$ to a and $\eta=0$ to 2π, one obtains a system of simultaneous ordinary differential equations of the form

$$\begin{aligned}&\sum_{m=0}^{M}\sum_{n=0}^{N}[\alpha_{mn}\ddot{C}_{mn}+\varepsilon_{mn}\ddot{S}_{mn}+\lambda_{mn}\dot{C}_{mn}\\&\quad+\mu_{mn}\dot{S}_{mn}+\phi_{mn}C_{mn}+\upsilon_{mn}S_{mn}]_{ql}\\&\quad+\Lambda_{Hql}u_H=f_{ql},\\&q=0,1,2,\ldots,M;\ l=0,1,2,\ldots,N.\end{aligned} \tag{6}$$

In the same way, substituting Eq.(4) into Eq.(1), multiplying by $rR_{ql}(r)\sin(l\eta)d\eta dr$ and integrating gives

$$\begin{aligned}&\sum_{m=0}^{M}\sum_{n=0}^{N}[\bar{\alpha}_{mn}\ddot{S}_{mn}+\bar{\varepsilon}_{mn}\ddot{C}_{mn}+\bar{\lambda}_{mn}\dot{S}_{mn}\\&\quad+\bar{\mu}_{mn}\dot{C}_{mn}+\bar{\phi}_{mn}S_{mn}+\bar{\upsilon}_{mn}C_{mn}]_{ql}\\&\quad+\bar{\Lambda}_{Hql}u_H=\bar{f}_{ql},\\&q=0,1,2,\ldots,M;\ 1,2,\ldots,N;\end{aligned} \tag{7}$$

where

$$\alpha_{mn}=\bar{\alpha}_{mn}=\langle R_{mn}^2\rangle\delta_{mq}\delta_{nl},$$

$$\varepsilon_{mn}=\bar{\varepsilon}_{mn}=0,$$

$$\lambda_{mn}=\bar{\lambda}_{mn}=\bar{c}\,\bar{k}_{mn}^4\langle R_{mn}^2\rangle\delta_{mq}\delta_{nl},$$

$$\mu_{mn}=-2n\bar{\Omega}\langle R_{mn}^2\rangle\delta_{mq}\delta_{nl},$$

$$\bar{\mu}_{mn}=2n\bar{\Omega}\langle R_{mn}^2\rangle\delta_{mq}\delta_{nl},$$

$$\phi_{mn}=(\bar{k}_{mn}^4-n^2\bar{\Omega}^2)\langle R_{mn}^2\rangle\delta_{mq}\delta_{nl}+\langle\sigma R_{mn}^{ql}\rangle\delta_{nl}+\frac{1}{\beta_l}\bar{k}_{\mathrm{air}}\langle C_{nl}R_{mn}^{ql}\rangle_i,$$

$$\bar{\phi}_{mn}=(\bar{k}_{mn}^4-n^2\Omega^2)\langle R_{mn}^2\rangle\delta_{mq}\delta_{nl}+\langle\sigma R_{mn}^{ql}\rangle\delta_{nl}+\bar{k}_{\mathrm{air}}\langle S_{nl}R_{mn}^{ql}\rangle_i,$$

$$\upsilon_{mn}=-n\bar{c}\,\overline{\Omega k}_{mn}^4\langle R_{mn}^2\rangle\delta_{mq}\delta_{nl}+\frac{1}{\beta_l}\bar{k}_{\mathrm{air}}\langle S_nC_lR_{mn}^{ql}\rangle_i,$$

$$\bar{\upsilon}_{mn}=n\bar{c}\,\overline{\Omega k}_{mn}^4\langle R_{mn}^2\rangle\delta_{mq}\delta_{nl}+\bar{k}_{\mathrm{air}}\langle C_nS_lR_{mn}^{ql}\rangle_i,$$

$$\Lambda_{Hql}=-\frac{1}{\beta_l}\bar{k}_{\mathrm{air}}R_{ql}(\bar{\xi})\cos l\eta_0,$$

$$\bar{\Lambda}_{Hql}=-\bar{k}_{\mathrm{air}}R_{ql}(\bar{\xi})\sin l\eta_0,$$

$$\langle R_{mn}^2\rangle=\int_{b/a}^{1}\bar{r}R_{mn}^2(\bar{r})d\bar{r},$$

$$\langle\sigma R_{mn}^{ql}\rangle=\int_{b/a}^{1}-\left[\frac{\partial}{\partial\bar{r}}\left(\bar{\sigma}_r\bar{r}\frac{\partial R_{ml}(\bar{r})}{\partial\bar{r}}\right)-\frac{l^2}{\bar{r}}\bar{\sigma}_\eta R_{ml}(\bar{r})\right]R_{ql}(\bar{r})d\bar{r},$$

$$\langle C_{nl}R_{mn}^{ql}\rangle_i=\cos n\eta_{0i}\cos l\eta_{0i}\,R_{mn}(\bar{\xi}_i)R_{ql}(\bar{\xi}_i),$$

$$\langle S_nC_lR_{mn}^{ql}\rangle_i=\sin n\eta_{0i}\cos l\eta_{0i}\,R_{mn}(\bar{\xi}_i)R_{ql}(\bar{\xi}_i),$$

$$\langle C_nS_lR_{mn}^{ql}\rangle_i=\cos n\eta_{0i}\sin l\eta_{0i}\,R_{mn}(\bar{\xi}_i)R_{ql}(\bar{\xi}_i),$$

$$\langle S_{nl}R_{mn}^{ql}\rangle_i=\sin n\eta_{0i}\sin l\eta_{0i}\,R_{mn}(\bar{\xi}_i)R_{ql}(\bar{\xi}_i),$$

$$\beta_l=\begin{cases}2 & \text{for } l=0\\ 1 & \text{for } l\neq 0\end{cases},$$

$$\delta_{ij}=\begin{cases}1 & \text{for } i=j\\ 0 & \text{for } i\neq j\end{cases},$$

$$f_{ql}=\begin{cases}-[\bar{G}_a\langle\bar{r}R_{ql}\rangle\delta_{l0}+\bar{G}_p\langle\bar{r}^2R_{ql}\rangle\delta_{l1}]\sin\bar{w}T & \text{for } 0\le T\le\bar{\tau},\\ 0 & \text{for } \bar{\tau}<T\end{cases}$$

$$\bar{f}_{ql}=0. \tag{8}$$

Similarly, substitution of Eq.(4) into Eq.(2) leads to

$$\begin{aligned}&\alpha_H\ddot{u}_H+\phi_Hu_H\\&\quad+\sum_{m=0}^{M}\sum_{n=0}^{N}[\Phi_{mn}C_{mn}+\Psi_{mn}S_{mn}]=f_H,\end{aligned} \tag{9}$$

where

$$\alpha_H=\bar{m},$$

$$\phi_H=\bar{k}+\bar{k}_{\mathrm{air}},$$

$$\Phi_{mn}=-\bar{k}_{\mathrm{air}}R_{mn}(\bar{\xi})\cos n\eta,$$

$$\Psi_{mn}=-\bar{k}_{\mathrm{air}}R_{mn}(\bar{\xi})\sin n\eta,$$

$$f_H=\begin{cases}-\bar{m}[\bar{G}_a+\bar{G}_p\bar{\xi}\cos\eta_0]\sin\bar{\omega}T & \text{for } 0\le T\le\bar{\tau}.\\ 0 & \text{for } \bar{\tau}<T\end{cases} \tag{10}$$

The nondimensional parameters introduced in the above equations are as follows.

$$\begin{aligned}&T=\left(\frac{D}{\rho ha^4}\right)^{\frac{1}{2}}t, && \bar{\tau}=\left(\frac{D}{\rho ha^4}\right)^{\frac{1}{2}}\tau,\\&\bar{\sigma}_r=\left(\frac{ha^2}{D}\right)\sigma_r, && \bar{\sigma}_\eta=\left(\frac{ha^2}{D}\right)\sigma_\eta,\\&\bar{\Omega}=\left(\frac{\rho ha^4}{D}\right)^{\frac{1}{2}}\Omega, && \bar{\omega}=\left(\frac{\rho ha^4}{D}\right)^{\frac{1}{2}}\omega,\\&\bar{c}=\left(\frac{D}{\rho ha^4}\right)^{\frac{1}{2}}c, && \bar{m}=\frac{1}{\rho ha^2\pi}m,\\&\bar{k}=\frac{a^2}{D\pi}k, && \bar{k}_{\mathrm{air}}=\frac{a^2}{D\pi}k_{\mathrm{air}},\\&\bar{r}=\frac{r}{a}, && \bar{\xi}=\frac{\xi}{a}.\end{aligned} \tag{11}$$

With the use of matrix expressions, Eqs.(6), (7) and (9) are rewritten as

$$\boldsymbol{M}\ddot{\boldsymbol{X}}+\boldsymbol{C}\dot{\boldsymbol{X}}+\boldsymbol{K}\boldsymbol{X}=\boldsymbol{F}, \tag{12}$$

where $\boldsymbol{X}$ is a matrix of C_{mn}, S_{mn} and u_H, $m=0,1,2,\ldots,M$; $n=1,2,\ldots,N$. In the following, the Newmark β method is introduced to obtain the transient response of the system from Eq.(12). To this end, Eq.(12) is further discretized in time as

$$\begin{aligned}&\left[\boldsymbol{M}+\frac{1}{2}(\Delta t)\boldsymbol{C}+\beta(\Delta t)^2\boldsymbol{K}\right]\boldsymbol{X}_{s+1}\\&\quad=(\Delta t)^2[\beta\boldsymbol{F}_{s+1}+(1-2\beta)\boldsymbol{F}_s+\beta\boldsymbol{F}_{s-1}]\\&\quad+[2\boldsymbol{M}-(1-2\beta)(\Delta t)^2\boldsymbol{K}]\boldsymbol{X}_s\\&\quad-\left[\boldsymbol{M}-\frac{1}{2}(\Delta t)\boldsymbol{C}+\beta(\Delta t)^2\boldsymbol{K}\right]\boldsymbol{X}_{s-1}.\end{aligned} \tag{13}$$

Substituting the $\boldsymbol{X}$ determined from Eqs.(13) into Eq.(4) gives the solutions both for the displacement of disk u and that of head u_H.

3. Numerical Results

Numerical results that follow are for a 3.5″ hard disk rotating at 3 600 rpm, the physical parameters of which are listed in Table 1. The parameters of the R/W head in Table 2 were quoted from Ref. (6)-(8).

Since the value of the equivalent air film stiffness k_{air} depends on the floating space between the R/W head and the disk surface, and on the shape of the head slider, two extreme values (lower and upper bounds) were considered in the example. The series terms in Eq.(4) were considered up to $M=3$ and $N=6$. Hereinafter, the mode of vibration with m nodal circles and n nodal diameters will be denoted by the symbol (m, n).

Figure 2 shows the variations of the natural frequencies as functions of the rotation speed Ω. Figure 2(a) is for the case when the stiffness k_{air} is zero, Fig. 2(b) the case of $k_{air}=1\times10^5$N/m, and Fig. 2(c) the case of $k_{air}=5\times10^5$ N/m. In the figures, the broken line shows the natural frequency of the R/W head, and the solid lines the frequencies of the rotating disk. It is seen from the figures that the natural frequency of the head f_{head} is about 30 Hz in Fig. 2(a), and 3 kHz and 5.6 kHz in Figs. 2(b) and(c), respectively, i.e. f_{head} is strongly dependent on the air film stiffness k_{air}. The frequencies of the disk, on the other hand, are not significantly affected by the stiffness k_{air}. The frequency of the (0, 0) mode is about 1 kHz at $\Omega=0$. It becomes higher with an increase of the rotation speed. However, the increase is not significant, and it is less than 1% at 3 600 rpm. Every mode other than (0, 0) has two natural frequencies for non-zero rotation speeds as evident from the (0, 3) curves shown in the figure. The upper curve is the frequency of a flexural wave rotating in the same direction as the disk rotation, while the lower curve is the frequency of a wave travelling in the opposite direction to the disk rotation.

Table 1 Physical parameters of hard disks

Outer radius	a	(m)	47.5×10^{-3}
Inner radius	b	(m)	15.5×10^{-3}
Thichness	h	(m)	1.25×10^{-3}
Young's module	E	(N/m^2)	7.06×10^{10}
Density	ρ	(Kg/m^3)	2.66×10^3
Poisson's ratio	ν		0.33
Revolution speed	Ω	(rad/s)	377.0 (3600 rpm)

Table 2 Physical parameters of R/W head

	Mass m (Kg)	Stiffness k (N/m)	Air Stiffness k_{air} (N/m)	Floating Space (μm)
Ref.6	3.43×10^{-4}	10.8	1-5 $\times10^5$	0.50
	3.06×10^{-4}	10.8	—	0.65
Ref.7	—	—	2-4 $\times10^5$	0.30
Ref.8	2.35×10^{-4}	14.7	—	—
	1.57×10^{-4}	7.35	—	—
This study	3.00	10.0	1-5 $\times10^5$	—

The following figures show the transient response of the disk-head system when it is subjected to an impulsive acceleration. The results are obtained by the Newmark β method with $\beta=1/4$ and $\Delta t=0.02$ ms.

Figure 3 shows the time response of the spinning disk-head system when it is subjected to an axial half-sine shock pulse of peak acceleration $5g$(49 m/s^2). The results are shown for the point on the disk $(\bar{r}, \eta)$ $=(0.7, 0)$ and the damping coefficient $c=1.406^{-6}$s. The vertical dot-dashed line in the figures shows the time when the system acceleration in the axial direction ceases. The duration of the pulse is (a) $\tau=0.1$ ms, (b) $\tau=1$ ms and (c) $\tau=11$ ms. The solid line shows the response of the disk and the broken line the displacement of the head. The parameters of the head are $m=3\times10^{-4}$kg, $k=10$ N/m and $k_{air}=1\times10^5$N/m. It was assumed that the initial displacements of the head and the disk are both zero at $t=0$. It is found that the head vibrates inphase with the rotating disk at the frequency of about 1 kHz, which is the (0, 0) mode natural frequency of the rotating disk. The natural frequency of the head in this case is about 3 kHz as

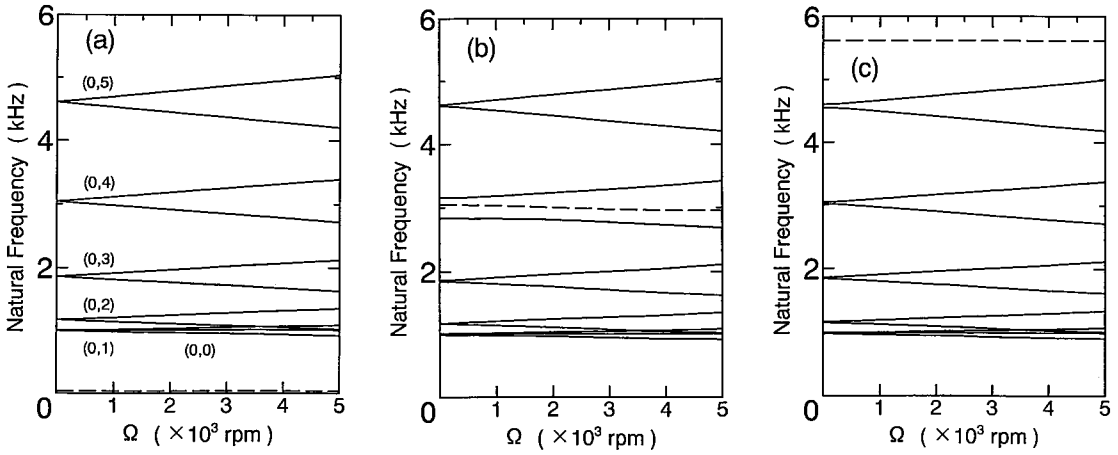

Fig. 2 Natural frequencies of 3.5″ hard disk-head system versus rotation speed. $m=3\times10^{-4}$kg, $k=10$ N/m, (a) $k_{air}=0$, (b), $k_{air}=1\times10^5$N/m, (c) $k_{air}=5\times10^5$N/m

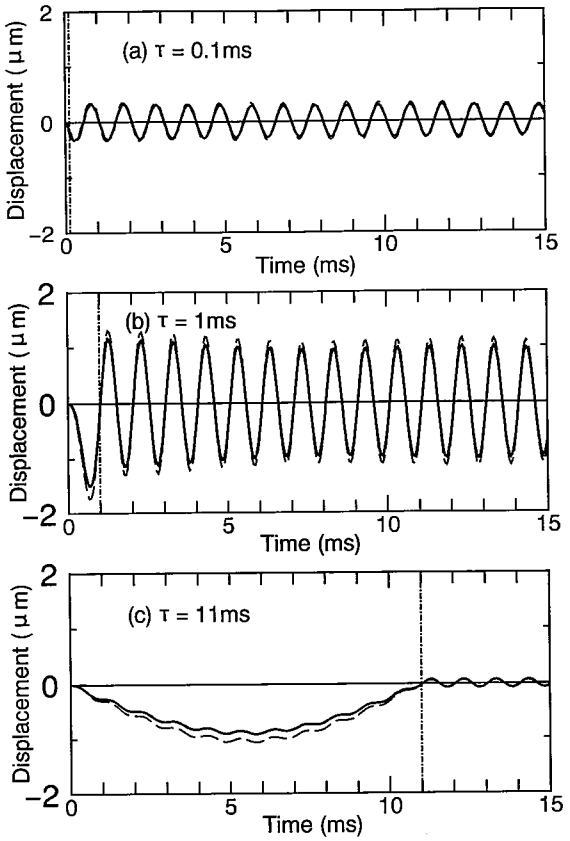

Fig. 3 Displacement response of spinning disk-head system to axial excitation. $m=3\times10^{-4}$kg, $k=10$ N/m, $k_{air}=1\times10^{5}$N/m, $G_a=5$ g, $G_p=0$, $(r/a, \eta)=(0.7, 0)$

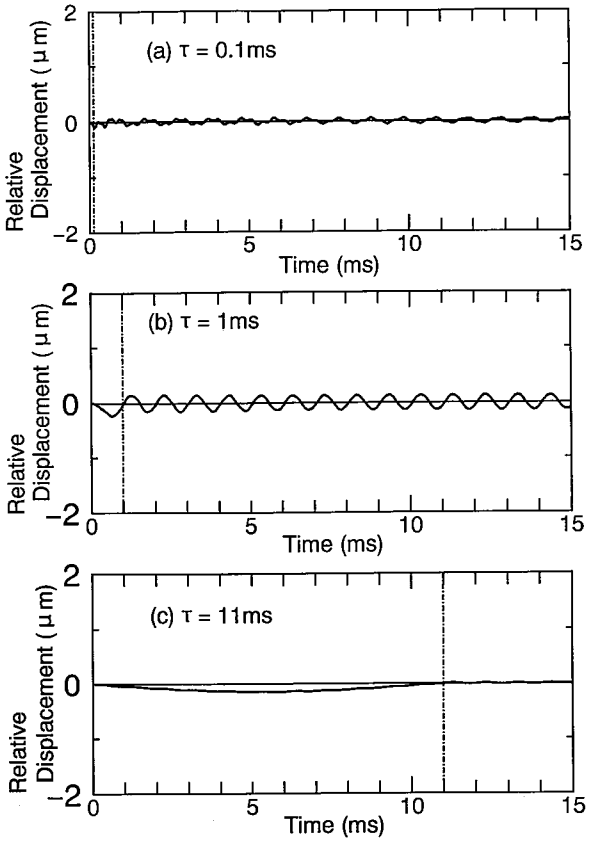

Fig. 4 Relative displacement of head to disk for the system of Fig. 3

evident from Fig. 2(b), which means that the head is not vibrating at its own natural frequency but it is simply following the vibration of the disk. This is attributed to the fact that the inertia of the disk is much greater than that of the head, and that the stiffness of the air film k_{air} is also greater than the head arm stiffness k. The figures also show that the displacements of both the disk and the head take peak values before or shortly after the system was released from the disturbance, and that the peak values increase or decrease depending on the duration of the input impulse, which leads to an understanding that there is a duration for which the peak displacement takes a maximum.

Figure 4 shows the variation of the relative displacement, which was obtained from Fig. 3 by subtracting the disk displacement from the head displacement. Since the initial displacements of the head and the disk were set equal to zero in the numerical calculation, the relative displacement sometimes takes a negative value as observed from the figure. However, there is an initial floating space between the head slider and the disk due to the air film between them. Then, if the relative displacement is less than the value of the initial space, the head-disk system will experience no impact during operation. This condition is satisfied for the case of Fig. 4 since the initial space between the head and the disk is 0.5 - 0.65 μm (6,7) and the negative maximum of the peak relative displacement is −0.23 μm. Thus the disk-head system has no crash and is safe under an impulsive acceleration of $5g$. It is also noted that the peak values of the negative relative displacement increase or decrease depending on the value of the input duration. Thus there is a duration for which the peak relative displacement takes a negative maximum.

Figures 5 - 8 show the variations of the peak displacement and the peak negative relative displacement as functions of the input duration. Figures 5 and 7 are the variations of peak displacement for the axial and the pitching excitations, and Figs. 6 and 8 are the corresponding results for the peak negative relative displacement. The abscissa of the figures is the non-dimensional duration of impulse τ/τ_{00}, where τ_{00} is the half-period of the (0, 0) vibration mode. For the 3.5″ hard disk under consideration, the frequency of (0, 0) mode is $f_{00}=1$kHz, and the half period is given by $\tau_{00}=1/2f_{00}(=0.5$ ms). It is found from Figs. 5 and 7 that both the head peak displacement and that of the disk take maxima at $\tau\simeq1.5\tau_{00}$. A similar result has already been found in the analysis of the rotating disk system

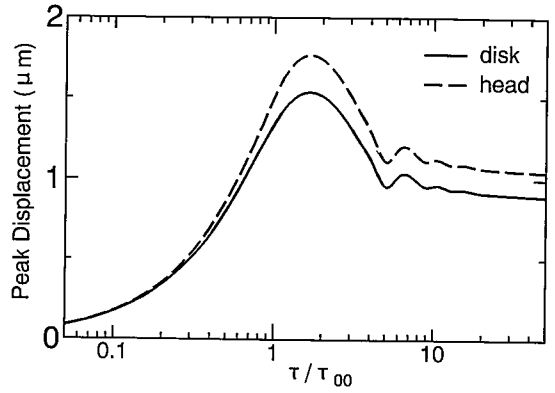

Fig. 5 Variation of peak displacements of disk and head versus input acceleration duration (axial excitation). $m=3\times10^{-4}$kg, $k=10$N/m, $G_a=5$ g, $G_p=0$

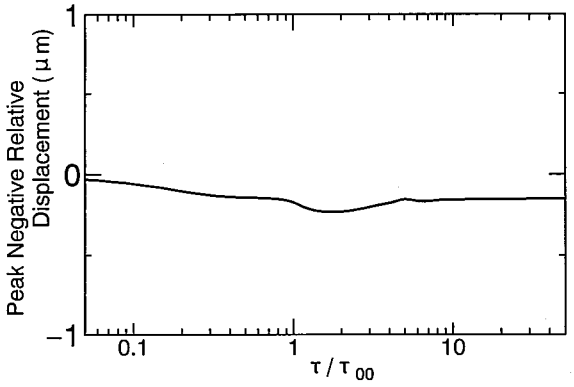

Fig. 6 Variation of peak negative relative displacement of head to disk for the system of Fig. 5

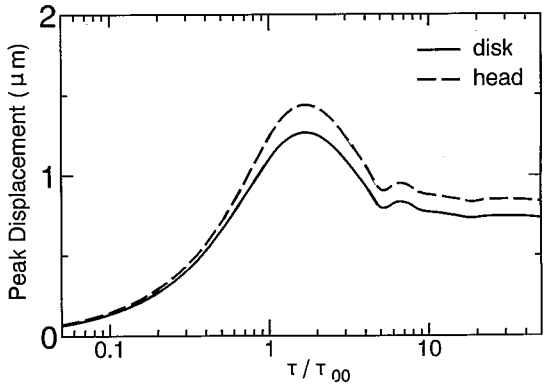

Fig. 7 Variation of peak displacements of disk and head versus input acceleration duration (pitching excitation). $m=3\times10^{-4}$kg, $k=10$ N/m, $k_{air}=1\times10^5$ N/m, $G_a=0$, $G_p=5$ g

without a head (see Ref. (9)). It is seen from Figs. 6 and 8 that the peak negative relative displacement takes a maximum again at $\tau\simeq1.5\tau_{00}$.

The half-sine acceleration with a duration of 11 ms is currently commonly used by computer manufacturrs as a standard input for the shock test of disk drive units. The figures given above show that the shock pulse with a duration 11 ms produces only

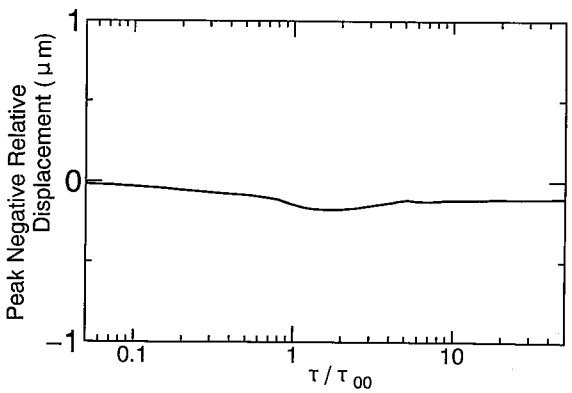

Fig. 8 Variation of peak negative relative displacement of head to disk for the system of Fig. 7

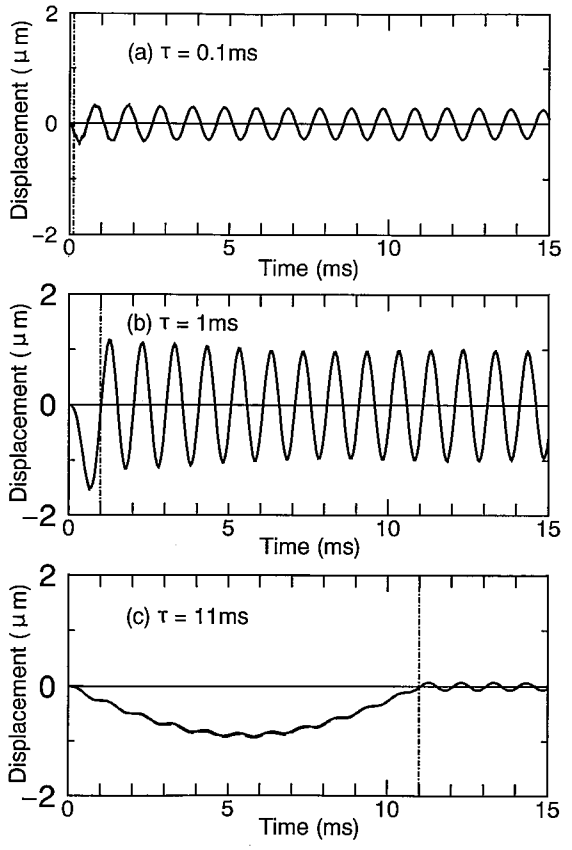

Fig. 9 Displacement response of spinning disk-head system with high air film stiffness $k_{air}=5\times10^5$ N/m. $m=3\times10^{-4}$kg, $k=10$ N/m

60 - 70% of the maximum displacement that may appear in the disk-head assembly.

Figure 9 shows the displacement response for the case of $k_{air}=5\times10^5$N/m which is the upper bound of the air film stiffness given in Table 2. By comparison with Fig. 3 it is seen that an increase of the air stiffness decreases the difference in displacement between the head and the disk, which means that the air stiffness plays an important role in the shock-proof design of the head-disk assembly. There are

three parameters that are involved in the design of the disk-head assembly. They are the mass and the stiffness of the read/write head-arm system, m and k, and the stiffness of the air film k_{air}. Among these parameters, the control of the air film stiffness requires a detailed discussion depending on the optimum design of the head slider, which is beyond the scope of this paper. In the following, attention will be focused on the optimum values of the stiffness of the head arm k.

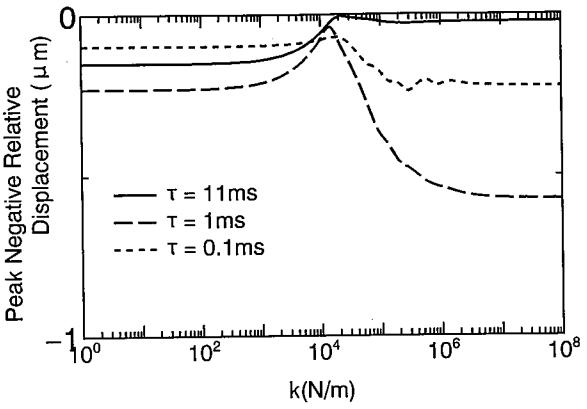

Fig. 10 Variation of peak negative relative displacements of head to disk versus stiffness of head arm k (axial excitation). $m=3\times10^{-4}$kg, $k_{air}=1\times10^5$ N/m

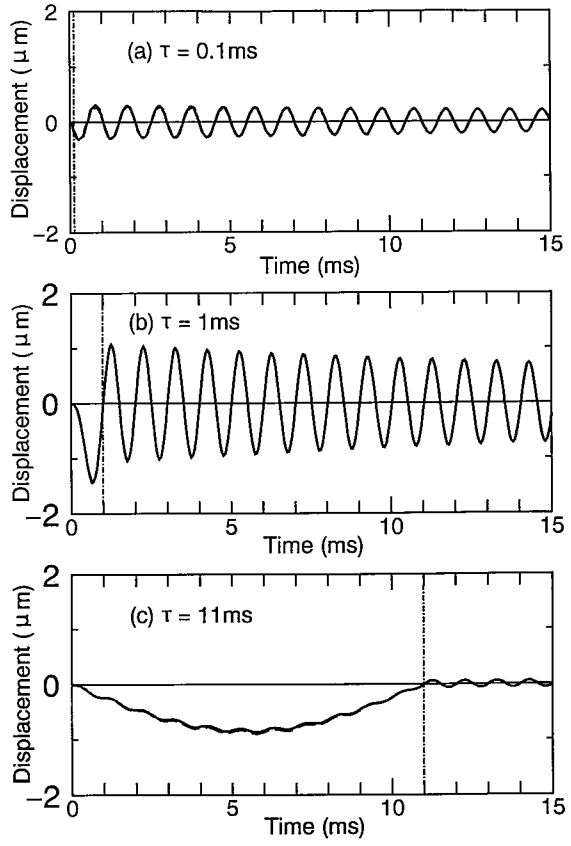

Fig. 11 Displacement response of spinning disk-head system with optimal stiffness $k=1.3\times10^4$N/m. $m=3\times10^{-4}$kg, $k_{air}=1\times10^5$N/m

Figure 10 shows the variation of the peak negative relative displacement as a function of the head arm stiffness k. In the figure, the solid line shows the result when the duration of input impulse is $\tau=11$ ms, the dashed line the case of $\tau=1$ ms, and the dotted line the case $\tau=0.1$ ms. It is clear from the figure that there exist some values of k that maintain the peak negative relative displacement minimum and keep the space between the head and the disk constant. It is seen from the figure that the optimal value of k is $(1\sim2)\times10^4$N/m, which is on the order of one-tenth of the air film stiffness $k_{air}(=1\times10^5$N/m). Figure 11 shows the displacement response when k is 1.3×10^4N/m. Comparing with the case of $k=10$ N/m (Fig. 3), it is seen that the difference is displacement between the head and the disk has been greatly reduced for $k=1.3\times10^4$N/m. Furthermore, comparison of Fig. 11 with Fig. 9 shows that the results obtained are almost the same in both cases, which implies that the stiffness of head has little effect on the head tracking ability to the disk surface when the air film stiffness is k_{air} sufficiently high.

Figure 12 shows the variations of peak negative relative displacement as functions of the input duration. The solid line is the result of Fig. 11 and the broken line that of Fig. 6. It is observed that the negative peak displacement for the case of optimal stiffness $k=1.3\times10^4$N/m is smaller than the displacement for $k=10$ N/m regardless of the value of τ under consideration. Thus, it is said that the introduction of optimal k is effective in preventing the impact of the head to the disk surface.

Figure 13 is the result obtained by reducing the air film stiffness from $k_{air}=1\times10^5$N/m to 1×10^4N/m, and Fig. 14 that obtained by increasing the head mass from $m=3\times10^{-4}$kg to 3×10^{-3}kg. In both cases, the

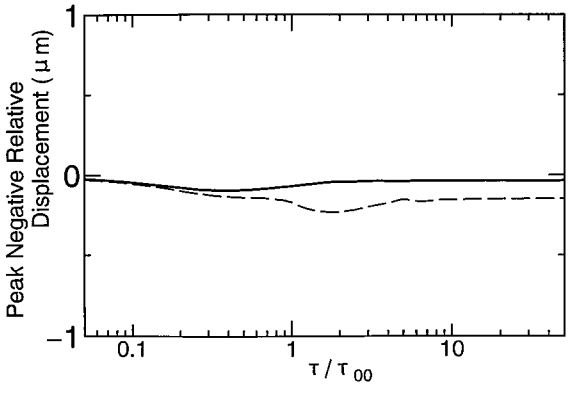

Fig. 12 Variation of peak negative relative displacement of head to disk versus input acceleration duration (axial excitation). $m=3\times10^{-4}$kg, $k=10$ N/m, —: $k=1.3\times10^4$N/m, ---: $k=10$ N/m

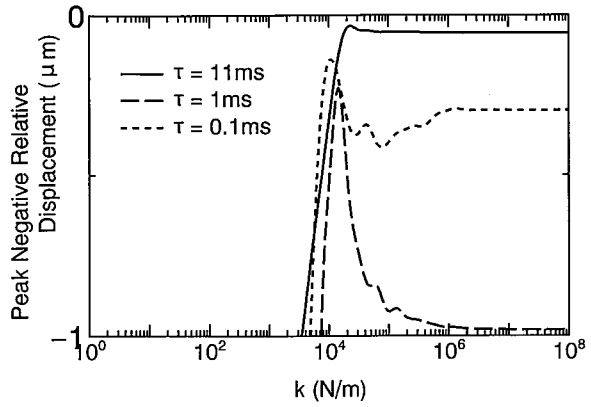

Fig. 13 Variation of peak negative relative displacements of head to disk versus stiffness of head arm k (axial excitation) with small air film stiffness. $k_{air}=1\times10^4$N/m. $m=3\times10^{-4}$kg

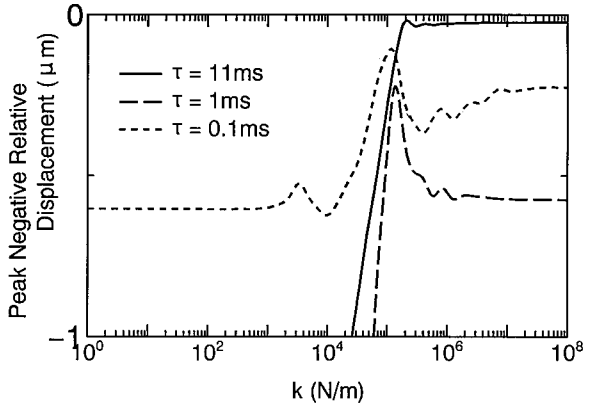

Fig. 14 Variation of peak negative relative displacements of head to disk versus stiffness of head-arm k (axial excitation) with large mass $m=3\times10^{-3}$kg. $k_{air}=1\times10^5$N/m

physical parameters, except k_{air} and m, are as given in Fig. 10. Comparison of Figs. 10, 13 and 14 shows that the optimal stiffness k is influenced less by the variation of the air film stiffness k_{air} than by the magnitude of the head mass m. This finding is interpreted as follows. For the case of $k_{air}=0$, the natural frequency of the head is given by $(1/2\pi)(k/m)^{1/2}$. When the natural frequencies of the heads given in Figs. 10, 13 and 14 are calculated from this equation, they are obtained as in Table 3. It is evident that the natural frequencies of the heads in those cases have the same value, 1.05 kHz. This is simply the (0, 0) mode frequency, f_{00}, of the spinning disk. This means that when the disk-head system is impulsively excited, the head and the disk will vibrate at the same frequency, and with the same phase angle. In this case, since the relative force between the head and the disk is small even if the air film stiffness k_{air} is introduced, then the influence of stiffness k_{air} is not significant either. The optimal stiffness of the head arm k is therefore determined from

Table 3 Natural frequencies of head for $k_{air}=0$

	Fig.10	Fig.13	Fig.14
Mass m ($\times10^{-4}$ Kg)	3	3	30
Stiffness k ($\times10^4$ N/m)	1.3	1.3	13
Natural Frequency of head (KHz)	1.05	1.05	1.05

$$f_{00}=\frac{1}{2\pi}\sqrt{\frac{k}{m}}. \tag{14}$$

Furthermore, it is evident from the comparison of Figs. 10, 13 and 14 that the region of stiffness that guarantees a safe operation of the system is narrowed if the air film stiffness k_{air} is very small or the head mass m is very large. In this case, if the stiffness k is not selected carefully, a possibility of impact would not be avoidable.

4. Conclusions

A theoretical study has been presented on the response of rotating hard disk-R/W head systems subjected to a half-sine shock acceleration in the axial and pitching directions. The results obtained can be summarized as follows.

(1) The peak negative relative displacement, which is a measure of the possibility of impact between the disk and the head, takes the maximum when the input shock duration is about 1.5 times the half-period of the fundamental (0, 0) mode. The shock pulse with a duration 11 ms, which is currently commonly used as a standard input for the shock test of disk drive units, prodces only 60 - 70% of the maximum displacement that may appear for the rotating disk.

(2) The difference in the displacement between the head and the disk becomes smaller with an increase of the air film stiffness. Thus the head slider should be designed so that the assembled system of the head and the disk has a high air film stiffness.

(3) The optimal head arm stiffness k is determined from

$$f_{00}=\frac{1}{2\pi}\sqrt{\frac{k}{m}},$$

where f_{00} is the fundamental (0, 0) mode frequency of the rotating disk, and m is the mass of the head.

(4) The durability of disk-head systems to the shock pulse can be evaluated by the method presented in this paper.

References

(1) Ono, K., Maeno, T. and Ebihara, T., A Study of Head to Media Interface in Flexible Disk, Trans. Jpn. Soc. Mech. Eng., (in Japanese), Vol. 52, No. 437, C(1986), p. 326.

(2) Chonan, S. and Jiang, Z. W., Dynamic Response of

Rotating Disks Subjected to Axial and Pitching Oscillations, Trans. Jpn. Soc. Mech. Eng., (in Japanese), Vol. 54, No. 502, C(1988), p. 1181.
(3) Jiang, Z. W., Chonan, S. and Abe, H., Dynamic Response of a Read/Write Head Floppy Disk System Subjected to Axial Excitation, Trans. ASME J. Vib. & Acoust., Vol. 112, (1990), p. 53.
(4) Honda, Y., Matsuhisa, H. and Sato, S., The Steady State Response of a Rotating Disk to a Concentrated Harmonic Force at a Space-Fixed Point, Trans. Jpn. Soc. Mech. Eng., (in Japanese), Vol. 54, No. 507, C(1988), p. 2610.
(5) Yano, S. and Kotera, T., Instability of the Vibrations of a Rotating Thin Disk due to an Additional Support, Archive of Applied Mechanics, Vol. 61, (1991), p. 110.
(6) Ono, S., Kogure, K. and Mitsuya, Y., Trans. Jpn. Soc. Mech. Eng., (in Japanese), Vol. 45, No. 391, C (1979), p. 356.
(7) Fukui, S., Kogure, K. and Mitsuya, Y., Trans. Jpn. Soc. Mech. Eng., (in Japanese), Vol. 51, No. 469, C (1985), p. 2291.
(8) Odaka, T., Tanaka, K., Takeuchi, Y. and Saitoh, Y., Dynamic Characteristics of Air-Lubricated Slider Bearing for Magnetic Disk Files, Trans. Jpn. Soc. Mech. Eng., (in Japanese), Vol. 53, No. 487, C(1987), p. 815.
(9) Chonan, S., Jiang, Z. W. and Takashima, K., Dynamic Characteristics of Hard Disks Subjected to Impulsive Excitation, Trans. Jpn. Soc. Mech. Eng., (in Japanese), Vol. 58, No. 548, C(1992), p. 1105.